Green Chemistry

Accepted Manuscript

ROYAL SOCIETY OF CHEMISTRY

www.rsc.org/greenchem

Journal Name

ARTICLE

Modified PEDOT by preparing N-doped reduced graphene oxide as potential bio-electrode coating material

Received 00th January 20xx,

Accepted 00th January 20xx

DOI: 10.1039/x0xx00000x

www.rsc.org/

Mengmeng Fan[a], Chunlin Zhu[a], Lin Liu[a], Qilu Wu[a], Qingli Hao[b], Jiazhi Yang[a], Dongping Sun[a]*

We successfully prepare poly (3, 4-ethylenedioxythiophene) (PEDOT)/N-doped reduced graphene oxide (N-rGO) by electrodeposition, post-reduction, and doping N atoms with microorganism (as green reagent) to modify PEDOT and resolve the exfoliation, fragment problems of pristine PEDOT. This modification greatly improves the electrochemical properties of PEDOT showing great potential for bio-electrode coating material which should have excellent electrochemical properties, stability and biocompatibility. The as-prepared PEDOT/N-rGO shows lower impedance, higher capacitive performance, cyclical stability than pristine PEDOT due to the doping of N-rGO. MTT assay demonstrates this modified PEDOT has good adhesion, cell viability and proliferation similar to pristine PEDOT. It indicates this modifying progress of PEDOT does not restrain the good biocompatibility of pristine PEDOT, which results from the doping of high biocompatible N-rGO by this green method. The wrinkled structure, residual oxygen containing functional groups and doping N atoms of N-rGO lead to forming fluctuant surface and increasing hydrophilicity of PEDOT, respectively, which increase specific surface area and cell adhesion in cell culture, respectively. Consequently, this modified PEODT improves electrochemical properties, resolves the exfoliation, fragment problems of pristine PEDOT, and meanwhile, still retains the high biocompatibility of pristine PEDOT, which is promising for bio-electrode coating material.

1. Introduction

Recent years, implantable biomedical devices have achieved great development in medicine field including diagnostics and monitoring,[1] drug delivery,[2-3] neurology,[4] orthopedic operation,[5] audiology and cardiology,[6] *etc*. One of most important factors to decide the performance of implanted device is the efficiency and reliability of an electrode.[7-8] Generally, a small size of the electrode can lower the damage to the tissue but it inevitably decreases the electrochemical performance and safety of the electrode,[9] for example increasing impedance and decreasing charge storage capacity. However, coating material plays a significant role to improve the performance of the electrode.

It has been reported that noble metals (Pt, Au, Ti, *etc*.) and Iridium oxide are widely used as the coating materials[10] but low charge storage capacity, weak bonding with electrode restricted their further application.[11-12] Conducting polymers, especially PEDOT,[13] is an ideal coating material of electrode.[14] PEDOT not only overcomes the drawbacks of conventional coating materials[15] but also possesses high biocompatibility[16] and stability in continuous operation.[17] However, the exfoliation and fragments of pristine PEDOT from electrode arouse the stability and safety problems during electrochemical oxidation-reduction procedure.[16] Therefore, the modification of PEDOT by doping other materials is an effective way to overcome above problems and simultaneously improves the electrochemical properties of pristine PEDOT.[18-19] Since PEDOT acts as the biological coating material, we significantly hope the doping material does not destroy the excellent biocompatibility of pristine PEDOT.

Recently, graphene or graphene oxide (GO) has been widely studied to act as the doping material due to its excellent electrical, mechanical, thermal and optical properties.[20-23] Nevertheless, GO possesses high cytotoxicity,[24-25] insulativity which decreases biocompatibility and conductivity of coating material.[26] Graphene has high hydrophobicity[27] leading to sharp piercing for membrane[28-29] or protein denaturation in cell culture.[30] However, N-doped reduced graphene oxide (N-rGO)[31-34] with high hydrophilicity[35] and electrical conductivity has been rarely reported for the modification of PEDOT. Furthermore, the doping N atoms of N-rGO are beneficial to cell adhesion, viability, proliferation.[35]

Generally, N-rGO is produced by chemical reducing GO with toxic reagents such as ammonia,[36] hydrazine hydrate,[37] urea[38] and melamine[39] which are harmful to biological application. Nevertheless, in this paper, we propose a green and mild method[40] using microorganism as green reducing, N doping

[a] Chemicobiology and Functional Materials Institute of Nanjing University of Science and Technology, Xiao Ling Wei 200, Nanjing, 210094, China. Fax: 86-25-84431939; Tel: 86-25-84315079; E-mail: sundpe301@163.com.
[b] Key Laboratory for Soft Chemistry and Functional Materials of Ministry Education, Nanjing University of Science and Technology, Xiao Ling Wei 200, Nanjing, Jiangsu, 210094, China.

Electronic Supplementary Information (ESI) available: [the polymerization mechanism of PEDOT/GO, AFM image of blank PEDOT, SEM images of cross section for blank PEDOT and PEDOT/N-rGO, Raman spectrums, FT-IR spectrums, FE-SEM images of HUVECs cultured for 72h]. See DOI: 10.1039/x0xx00000x

reagent to prepare higher biocompatible N-rGO as the doping material for modifying PEDOT.

To the best of our knowledge, this green preparing approach of N-rGO has not been used for modification of PEDOT. Consequently, we doped N-rGO into PEDOT by this green method, resolved the exfoliation and fragment problems, and simultaneously improved the electrochemical properties of pristine PEDOT. The greatest advantage for overall modifying progress is that it does not require any toxic chemical reagents.

2. Experimental

2.1 Electrodeposition of PEDOT/GO

The mixed solution composed of 0.01M 3, 4-ethylenedioxythiophene (EDOT) (Aladdin Industrial Corporation) and 2mgmL^{-1} GO (XFNano, China). The 10 ml above solution or 10 ml 0.01M blank EDOT solution was treated by ultrasonic for 20 min before polymerization to prepare PEDOT/GO or blank PEDOT, respectively. The solution was purged with nitrogen gas for 20 min. The constant current for polymerization was set 0.1 mA and the polymerization time was 1h unless otherwise stated. Platinum and Ag/AgCl acted as the counter electrode and reference electrode, respectively. After polymerization, the modified electrode was washed thoroughly with deionized water and dried at room temperature. The gold chip (as the electrode) was prepared by spraying Au on a small size glass slide.

2.2 Preparation of PEDOT/N-rGO and PEDOT/H-rGO

The obtained PEDOT/GO electrodeposited on a gold chip (0.8cm×1.5cm) was incubated with microorganism from microbial fuel cell for 72 hours at 30°C. The microbial fuel cell has been assembled for a long time in our laboratory. The microorganism was substituted for hydrazine hydrate to prepare PEDOT/H-rGO in a representative chemical preparing method of N-rGO. PEDOT/GO electrodeposited on a gold chip was sealed in a vacuum dryer filling with hydrazine hydrate gas at 50 °C for 12 hour. The chips were repeatedly washed with 10% hydrochloric acid, 80% ethanol and finally washed with deionized water until neutral pH.[41]

2.3 Morphology, composition and structure characteristics

The samples were characterized by a scanning electron microscope (SEM) (JEOL JSM-6700). SEM observations were conducted at an accelerating voltage of 15.0 kV. Field-emission scanning electron microscopy (FE-SEM) was performed with a microscope (FEI Quanta 250F). The Atomic Force Microscope (AFM) image was completed by Atomic force microscope (BRUKER Dimension Icon)

The X-ray photoelectron spectroscopy (XPS) spectra was completed by a RBD upgraded PHI-5000C ESCA system (Perkin Elmer) with Mg K radiation (h =1253.6 eV). The Fourier Transform Infrared Spectroscopy (FT-IR) analysis was conducted on a Bruker Model IFS 66v/s spectrophotometer. Raman spectra recorded from 0 to 5000 cm^{-1} on a Renishaw Invia Raman Microprobe using a 514 nm argon ion laser.

2.4 Electrochemical characteristics

The Electrochemical Impedance Spectroscopy (EIS) measurements were completed from 0.1 to 1.0×10^5 Hz in electrochemical workstation (Shanghai Chenhua CHI760C). The Cyclic voltammetry (CV) measurements were taken from −0.8V to 0.8V at a scan rate of 5 mVs^{-1} in 0.1 M KOH solution using an electrochemical workstation in a three-electrode with Pt electrode as the counter electrode and Ag/AgCl electrode as the reference electrode at room temperature. Unless otherwise specified, all the potentials are against Ag/AgCl as reference potential.

2.5 Cytotoxicity assay

3-(4, 5-dimethylthiazol-2-yl)-2, 5-diphenyltetrazolium bromide (MTT) assay was used to test cytotoxicity of material by human umbilical vein endothelial cells (HUVECs). HUVECs were cultured in Dulbecco's modified eagle medium (DMEM) supplemented with 10% fetal calf serum, 1% penicillin-streptomycin at 37°C in a humidified (5% CO_2, 95% air) atmosphere. The cells were planted in a 96-well microplate at a density of 3000 cells per well for MTT assays. The cells were exposed to different samples incubated at 37 °C for 24h or 72h. Then the medium was replaced by Hank's balancing buffer followed by addition of 20 mL MTT buffer (5 mgmL^{-1} of MTT in Hank's balancing buffer) and incubated for 4h. Then the medium was extracted and replaced with 100 mL dimethyl sulfoxide (DMSO) to dissolve the formazan salt. Cell viabilities were presented as the percentage of the absorbance of cells (cultured on materials) to the absorbance of cells on blank gold chip using the absorbance at 490 nm. Experiments were carried out in triplicate.[42]

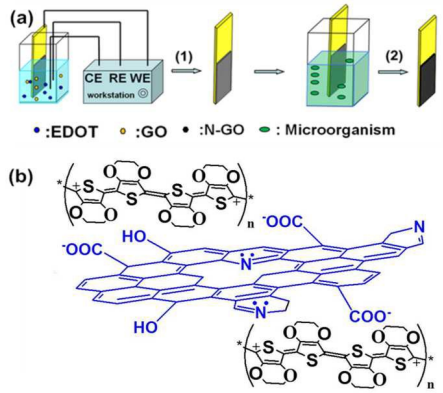

Fig. 1 The procedure of preparing PEDOT/N-rGO (a): (1) electrodeposition and (2) microbial reduction, N doping; the schematic representation of the structure of PEDOT/N-rGO (not drown in scale) (b).

3. Results and discussion

3.1 Preparation of PEDOT/N-rGO and morphology characteristics

The scheme of the proposed synthesis strategy of PEDOT/N-rGO (see Experimental section in detail) is shown in **Fig. 1**. Firstly, the gold chip was connected to the working electrode of electrochemical workstation to obtain PEDOT/GO by electrodeposition in the mixed electrolyte of GO and 3, 4-

ethylenedioxythiophene (EDOT).[20, 43-44] Then the chip was immersed into the microbial medium to get PEDOT/N-rGO (**Fig. 1b**) by post-reducing and N doping PEDOT/GO. The detailed electrodeposition mechanism of PEDOT/GO is given in Supporting Information (**Fig. S1**).

In order to observe the morphology of PEDOT with or without doping N-rGO, we got SEM, FE-SEM, AFM images. Firstly, the blank PEDOT comprises of many particles and small fragments on the surface showing typical porous structure of pristine PEDOT(**Fig. 2a, c**).[45] The AFM image also can affirm a lot of fragments on the surface of blank PEDOT (**Fig. S2**). The fragments and exfoliation probably occurs when continuous electrochemical stimulating. Meanwhile, the falling fragments cause safety problem and depress electrochemical property of pristine PEDOT.[16] To the contrary, the surface of PEDOT/N-rGO is covered with wrinkled sheets (**Fig. 2b)** stemming from the corrugated nature of graphene and the wrinkled structure effectively wraps the small fragments of PEDOT as shown in the internal of PEDOT/N-rGO at cracking area (**Fig. 2d**). The introduction of N-rGO can effectively prevent the exfoliation of PEDOT fragments. Therefore, PEDOT/N-rGO exhibits a more stable structure like "steel-concrete" (PEDOT as "concrete", and N-rGO as "steel"),[20] which can be affirmed by stability test using long-term Cyclic Voltammetry (CV) scanning. Noticeably, the fluctuant surface of PEDOT/N-rGO can effectively increase the contacting area for cell adhesion as demonstrated in AFM images (**Fig. 2e**, **f**) and the cross section of PEDOT/N-rGO on a gold chip (**Fig. S3)**.

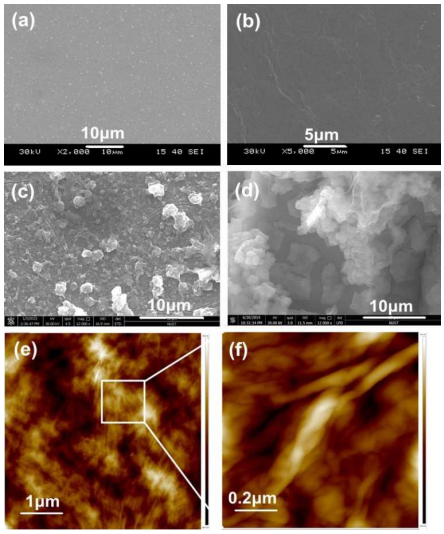

Fig. 2 SEM (a, b) and FE-SEM (c, d) images and AFM images (e, f) of blank PEDOT (a, c) and PEDOT/N-rGO (b, d, e, f). Image (d) was taken from an artificial cracking area of PEDOT/N-rGO.

3.2 Composition and structure characteristics

The XPS analysis was completed to affirm the successful N atoms doping, reduction of PEDOT/GO and obtain the configuration of N, S elements**.** Apart from mutual S, C and O elements, there are a ca. 3.6 % N elements emerged at 400eV (**Fig. 3a**) in PEDOT/N-rGO and the ratio of C/O increases from 2.34 of PEDOT/GO to 2.96 of PEDOT/N-rGO, which indicates the successful N doping and the reduction of oxygen containing functional groups of GO, respectively. Moreover, the Raman analysis also demonstrates GO has been deoxygenated in PEDOT/N-rGO according to the decreasing ratio of I_D/I_G (**Fig. S4**, decreasing from 1.46 to 1.33).[46] The reduction of oxygen containing functional groups can restore sp^2 carbons in graphene plane, which decreases defects and increases conductivity.

Furthermore, we can get the N atoms configuration in the high resolution N1s peak. The two peaks located at 398.6 eV and 400.1 eV are assigned to pyridinic-N and pyrrolic-N,[47] respectively (**Fig. 3b**). Pyridinic-N generally distributes on the edge and basal plane of graphene, which offers a significant number of active sites[48-49] and is beneficial to cell adhesion.

As shown in **Fig. 3c**, the peak at 162.2 eV can be assigned to the S–N bond due to the combination of N atoms of N-rGO with S atoms of PEDOT. PEDOT is expected to act as the extended resonating electron-transfer component. The S–C bond at 163.5 eV refers to the inner chemical bond of S and C in PEDOT.[50-51] Furthermore, the peak appearing at 167.2 eV results from neutralizing the positive charge of S atoms in PEDOT chains, which may be due to the electronegative oxygen atoms in oxygen containing functional groups of N-rGO withdrawing the electron density of the S atoms of PEDOT.[52-54] Therefore, the peak deconvolution of S indicates intact PEDOT structure and the strong interaction of two components in PEDOT/N-rGO.

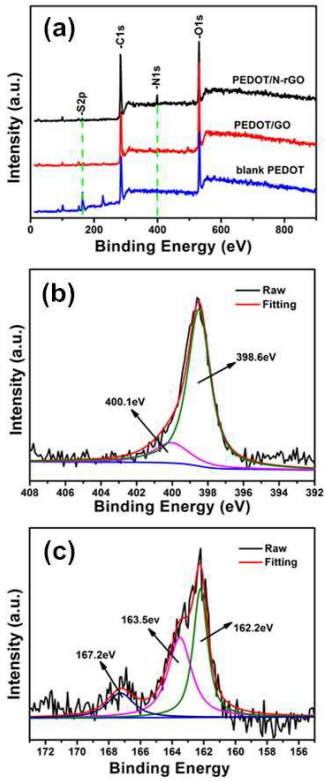

Fig. 3 Survey XPS spectrums of blank PEDOT, PEDOT/GO, PEDOT/N-rGO (a), and peak deconvolution of N1s and S2p core level of PEDOT/N-rGO (b, c)

Combined with the similar research,[55] the Raman spectrum analysis, the FT-IR analysis (**Fig. S4** and **S5**), it can be inferred that the π-π interaction between graphene plane and thiophene rings of PEDOT backbone plays a main role for the interconnection of two components. In addition, the rest of oxygen containing functional groups (especially, carboxyl)[20] and the doping N atoms (especially, pyridinic-N with a localized lone pair of electrons) of N-rGO are usually negatively charged.[56] The former is mainly responsible for negative charge of N-rGO owing to the abundant residue of oxygen containing functional groups. To the contrary, PEDOT is positively charged.[20] Therefore, PEDOT/N-rGO also includes the electrostatic interaction between PEDOT and N-rGO in **Fig. 1b**.[57-58]

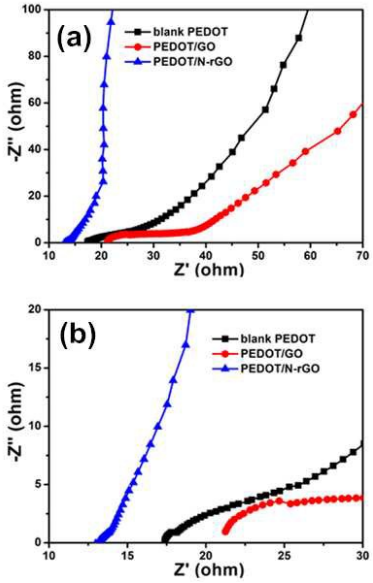

Figure 4. Nyquist plots (a) and expanded Nyquist plots (b) at high frequency for: blank PEDOT, PEDOT/GO and PEDOT/N-rGO.

3.3 Electrochemical characteristics

Impedance property is one of most important parameters for electrode coating material. As shown the EIS spectra in **Fig. 4**, the three Nyquist plots show small arcs in the high frequency and straight lines in the low frequency (**Fig. 4a**). The intercept with the Z' axis (real impedance axis) can be used to represent the intrinsic Ohmic resistance of the internal resistance or equivalent series resistance of the electrode material and electrolyte.[59] Compared to blank PEDOT (17.5 Ω) and PEDOT/GO (21.3 Ω), PEDOT/N-rGO has the lowest value (13.5 Ω) (**Fig. 4b**) which suggests that the conductivity of PEDOT is effectively improved by the doping of N-rGO. Furthermore, the steeper gradient of PEDOT/N-rGO in the low frequency indicates faster ion diffusion and more suitable for capacitor,[20] which is a good property for electrical stimulation of electrode.[60] The above improved impedance property of modified PEDOT attributes to the good electrical conductivity of N-rGO and interconnected structure of PEDOT/N-rGO which reduce the ion transport resistance and minimize the ion diffusion distance, respectively.[61]

The CV measurements were carried out to explore the electrochemical stability and the change of charge storage capacity of PEDOT after doping N-rGO. The enhanced electrochemical stability of PEDOT/N-rGO (**Fig. 5a**) is demonstrated by almost no changed CV curve after long-term CV scanning. To the contrary, the scanning area reduces a lot for blank PEDOT after CV scanning (**Fig. 5b**). The increasing stability of PEDOT/N-rGO can be attributed to N-rGO interconnecting and covering small fragments of PEDOT.[20] Apparently, PEDOT/N-rGO shows a more rectangular shape and larger scan area (**Fig. 5c**) which indicates the good capacitor behaviour during charge transfer procedure[20] and the increasing charge storage capacity, respectively.[62] The improved charge storage capacity of PEDOT/N-rGO results from the different interior properties: firstly, the sheet structure of N-rGO interconnects with the porous structure of PEDOT and secondly, N-rGO itself possesses a good pseudocapacitive behaviour, abundant active sites, high electrical conductivity.[63]

The contact angles were measured to study the change of hydrophilicity of PEDOT with or without doping N-rGO. The value of contact angle for PEDOT/N-rGO (67.3°) is between that of blank PEDOT (87.5°) and that of PEDOT/GO (50.6°) as shown in **Fig. 5d-f**. The hydrophilicity of PEDOT is obviously enhanced by doping N-rGO, which attributes to the residue of oxygen containing functional groups and the doping N atoms in N-rGO. The increasing hydrophilicity is beneficial to protein adsorption in cell culture.[35] Compared to PEDOT/GO, PEDOT/N-rGO shows a lower hydrophilicity indicating that the oxygen containing functional groups in PEDOT/GO are effectively reduced by microorganism because the reduction of oxygen containing functional groups can decrease the hydrophilicity of material.

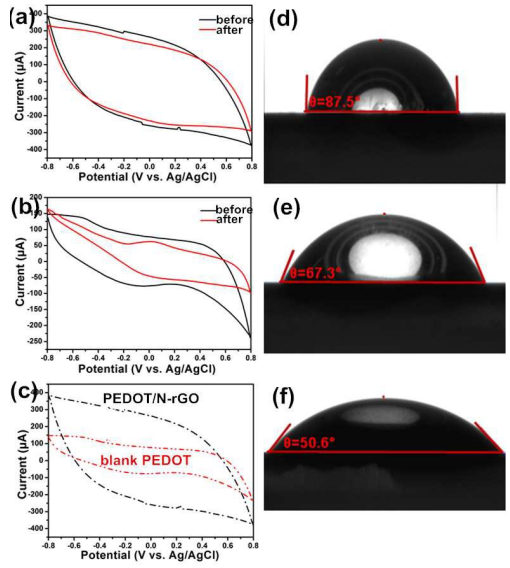

Figure 5. CV scanning curves before and after 200 cycles at rate of 5mVs^{-1} in N_2-saturated KOH solution (0.1M) (a=PEDOT/N-rGO and b=blank PEDOT) and the comparison of CV scanning area of samples (c); contact angles (d= blank PEDOT, e=PEDOT/N-rGO, and f= PEDOT/GO).

3.4 Cytotoxicity assay

MTT assay[64-65] and FE-SEM images were completed to investigate biocompatibility of this modified coating material by human umbilical vein endothelial cells (HUVECs). In order to demonstrate higher biocompatibility of green preparing N-rGO than that of conventional chemical preparing N-rGO, chemical preparing PEDOT/N-rGO was prepared using hydrazine hydrate as reducing, N doping reagent and is defined as PEDOT/H-rGO (see Experimental section in detail).

Compared to PEDOT/GO (94%) and PEDOT/H-rGO (88%), PEDOT/N-rGO has the highest viability value (103%) approaching to that of blank PEDOT (110%) in **Fig. 6f**, which indicates that the green preparing N-rGO shows a lower cytotoxicity for modulating PEDOT. Moreover, it demonstrates that pristine PEDOT itself has excellent biocompatibility as reported by previous papers.[16]

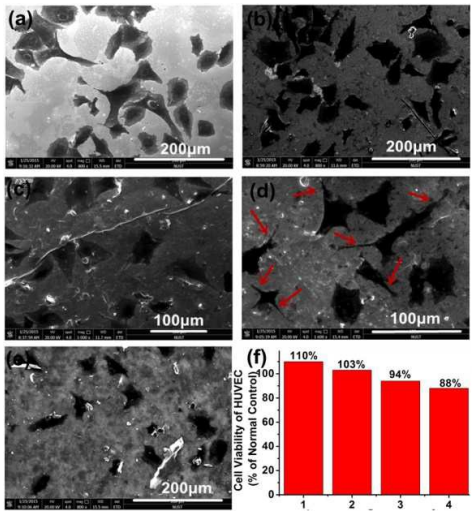

Figure 6. FE-SEM images of HUVECs: (a) blank gold chip; (b) blank PEDOT; (c) PEDOT/GO; (d) PEDOT/N-rGO; (e) PEDOT/H-rGO, prepared by reducing, N doping with hydrazine hydrate and (f) cell viability of HUVECs tested by MTT assay after 24h exposure to different samples (1=blank PEDOT; 2=PEDOT/N-rGO; 3=PEDOT/GO; 4=PEDOT/H-rGO)

In addition, the cells morphology on the surface of samples is also an important aspect to reflect the interaction between samples and cells. **Fig. 6a–e** shows the FE-SEM images of HUVECs adhered on the surfaces of different samples after 24h incubation. There are obvious pseddopods in spindly shape for the cells on the surface of PEDOT/N-rGO (**Fig. 6d**) similar to blank PEDOT (**Fig. 6b**). However, no obvious pseddopods appear on PEDOT/GO (**Fig. 6c**) and there are just relatively small and few pseudopods on PEDOT/H-rGO (**Fig. 6e**). The above different cell morphology indicates that PEDOT/N-rGO shows a higher performance in cell adhesion and growth than that of other modified PEDOT. Although many researchers have reported GO was a biocompatible material,[66-68] the green preparing N-rGO has a higher potential for modifying PEDOT in our study whose potential reasons are: 1) the N-rGO reduced by microorganism has a better biocompatibility owing to no usage of toxic reagents. 2) N-rGO has a lower geometrical damage to cells than that of GO.[69-70] 3) the doping N atoms can improve biocompatibility including cell viability, proliferation[35,71-72] and the nonspecific binding between the doping N atoms and cell surface proteins enhances cell adhesion force.[72-73] 4) the wrinkled surface and enhanced hydrophilicity of PEDOT/N-rGO increases cells contacting area.

We also further observed the cells morphology cultured on PEDOT/N-rGO and PEDOT/H-rGO for 72h. It shows that the cells on PEDOT/N-rGO connect together forming obvious vascular model *in vitro* (**Fig. S6a**). To the contrary, the cells on PEDOT/H-rGO just[74] have low cell density with less spreading (**Fig. S6b**). The above cell morphology suggests that the cells on PEDOT/N-rGO have a higher proliferation. Therefore, we affirm that the green preparing N-rGO has a higher biocompatibility than that of chemical preparing N-rGO.

4. Conclusions

It is demonstrated that PEDOT/N-rGO has enhanced electrochemical properties including low impedance, high electric capacity, and high stability. N-rGO sheets cover PEDOT fragments by π-π and electrostatic interaction, which effectively resolves exfoliation problem of pristine PEDOT. Meanwhile, the corrugated nature of N-rGO and the oxygen, nitrogen containing functional groups of N-rGO leads to forming fluctuant surface and increasing hydrophilicity of PEDOT, respectively, which are beneficial for cell adhesion. Compared to the other modified PEDOT, PEDOT/N-rGO has the highest biocompatibility approaching to that of pristine PEDOT, which can be attributed to high biocompatible N-rGO and no using any toxic chemical reagents in overall modifying progress. Therefore, we develop a rapid, environmentally friendly and efficient modifying approach which makes PEDOT a potential candidate as bio-electrode coating material.

Acknowledgements

This work was supported by “National Natural Science Foundation of China (Nos. 51272106, 21103092)”, “Research Fund for the Doctoral Program of Higher Education of China (RFDP) (No.20123219110015)”, Program for NCET-12-0629 and Qing Lan Project, “The Fundamental Research Funds for the Central Universities (No. 30920130121001, 30920130111003)” and “A Project Funded by the Priority Academic Program Development of Jiangsu Higher Education Institutions (PAPD, China)”, “Synergetic Research Center for Advanced Micro-Nano-Materials and Technology of Jiangsu Province”, “Advanced Catalysis and Green Manufacturing Collaborative Innovation Center".

Notes and references

1 C. A. Cordeiro, M. G. de Vries, W. Ngabi, P. E. Oomen, T. I. F. H. Cremers and B. H. C. Westerink, *Biosens. Bioelectron.,* 2015, *67* (0), 677-686.
2 Y. Zhu and L. Liao, *J. Nanosci. Nanotechno.,* 2015, *15* (7), 4753-4773.

3 M. Zheng, P. Gong, C. Zheng, P. Zhao, Z. Luo, Y. Ma and L. Cai, *J. Nanosci. Nanotechno.* 2015, *15* (7), 4792-4798.
4 V. Castagnola, E. Descamps, A. Lecestre, L. Dahan, J. Remaud, L. G. Nowak and C. Bergaud, *Biosens. Bioelectron.,* 2015, *67* (0), 450-457.
5 Z. Changhong, L. Xiuzhen, Z. Carl and L. Johan, *Biomed. Mater.,* 2015, *10* (1), 015019.
6 Y. Huang, J. F. Kong and S. S. Venkatraman, *Acta Biomater.,* 2014, *10* (3), 1088-1101.
7 S. F. Cogan, *Annu. Rev. Biomed. Eng.*, 2008**,** *10* (1), 275-309.
8 J. Mehdi, L. S. John, W. Christoph and R. C. Jeffrey, *J. Neural Eng.*, 2015, *12* (1), 011001.
9 W. M. Grill, S. E. Norman and R. V. Bellamkonda, *Annu. Rev. Biomed. Eng.*, 2009, *11* (1), 1-24.
10 D. R. Merrill, M. Bikson and J. G. R. Jefferys, *J. Neurosci. Meth.*, 2005, *141* (2), 171-198.
11 Y. Lu, T. Wang, Z. Cai, Y. Cao, H. Yang and Y. Y. Duan, *Sensor Actuat. B-Chem.*, 2009, *137* (1), 334-339.
12 S. F. Cogan, A. A. Guzelian, W. F. Agnew, T. G. H. Yuen and D. B. McCreery, *J. Neurosci. Meth.*, 2004, *137* (2), 141-150.
13 G. Greczynski, T. Kugler and W. R. Salaneck, *Thin Solid Films* 1999, *354* (1–2), 129-135.
14 M. R. Abidian and D. C. Martin, *Biomaterials,* 2008, *29* (9), 1273-1283.
15 R. A. Green, N. H. Lovell, G. G. Wallace and L. A. Poole-Warren, *Biomaterials,* 2008, *29* (24–25), 3393-3399.
16 M. R. Abidian, J. M. Corey, D. R. Kipke and D. C. Martin, *Small,* 2010, *6* (3), 421-429.
17 B. Winther-Jensen, O. Winther-Jensen, M. Forsyth and D. R. MacFarlane, *Science,* 2008, *321* (5889), 671-674.
18 K. J. Gilmore, M. Kita, Y. Han, A. Gelmi, M. J. Higgins, S. E. Moulton, G. M. Clark, R. Kapsa and G. G. Wallace, *Biomaterials,* 2009, *30* (29), 5292-5304.
19 X. Luo, C. L. Weaver, D. D. Zhou, R. Greenberg and X. T. Cui, *Biomaterials,* 2011, *32* (24), 5551-5557.
20 H.-C. Tian, J.-Q. Liu, D.-X. Wei, X.-Y. Kang, C. Zhang, J.-C. Du, B. Yang, X. Chen, H.-Y. Zhu, Y.-N. NuLi and C.-S. Yang, *Biomaterials,* 2014, *35* (7), 2120-2129.
21 Y. Ito, H. J. Qiu, T. Fujita, Y. Tanabe, K. Tanigaki and M. Chen, *Adv. Mater.,* 2014, *26* (24), 4145-4150.
22 Y. Zhu, S. Murali, W. Cai, X. Li, J. W. Suk, J. R. Potts and R. S. Ruoff, *Adv. Mater.,* 2010, *22* (35), 3906-3924.
23 B. K. Barman and K. K. Nanda, *Green Chem.,* 2015, *17* (2), 776-780.
24 J. Mao, R. Guo and L.-T. Yan, *Biomaterials,* 2014, *35* (23), 6069-6077.
25 M. C. Duch, G. R. S. Budinger, Y. T. Liang, S. Soberanes, D. Urich, S. E. Chiarella, L. A. Campochiaro, A. Gonzalez, N. S. Chandel, M. C. Hersam and G. M. Mutlu, *Nano Lett.,* 2011, *11* (12), 5201-5207.
26 V. Skákalová, V. Vretenár, Ľ. Kopera, P. Kotrusz, C. Mangler, M. Meško, J. C. Meyer and M. Hulman, *Carbon,* 2014, *72* (0), 224-232.
27 Y. B. Tan and J.-M. Lee, *J. Mater. Chem. A,* 2013, *1* (47), 14814-14843.
28 Y. Li, H. Yuan, A. von dem Bussche, M. Creighton, R. H. Hurt, A. B. Kane and H. Gao, *P. Natl. Acad. Sci.,* 2013, *110* (30), 12295-12300.
29 Y. Tu, M. Lv, P. Xiu, T. Huynh, M. Zhang, M. Castelli, Z. Liu, Q. Huang, C. Fan, H. Fang and R. Zhou, *Nat. Nano.* 2013, *8* (8), 594-601.
30 D. R. Lu and K. Park, *J. Colloid Interf. Sci.,* 1991, *144* (1), 271-281.
31 T. Van Khai, H. G. Na, D. S. Kwak, Y. J. Kwon, H. Ham, K. B. Shim and H. W. Kim, *J. Mater. Chem.,* 2012, *22* (34), 17992-18003.
32 M. Vikkisk, I. Kruusenberg, U. Joost, E. Shulga, I. Kink and K. Tammeveski, *Appl. Catal. B-Environ.*, 2014, *147*, 369-376.
33 S. Sandoval, N. Kumar, A. Sundaresan, C. N. R. Rao, A. Fuertes and G. Tobias, *Chem.-Eur. J.,* 2014, *20* (38), 11999-12003.
34 Y. Yoon, S. Seo, G. Kim and H. Lee, *Chem.-Eur. J.,* 2012, *18* (42), 13466-13472.
35 M. Guo, M. Li, X. Liu, M. Zhao, D. Li, D. Geng, X. Sun and H. Gu, *J. Mater. Sci.-Mater. M.*, 2013, *24* (12), 2741-2748.
36 G. Wang, W. Xing and S. Zhuo, *Electrochim. Acta,* 2013, *92*, 269-275.
37 D. Long, W. Li, L. Ling, J. Miyawaki, I. Mochida and S.-H. Yoon, *Langmuir,* 2010, *26* (20), 16096-16102.
38 W. Lei, W. Si, Q. Hao, Z. Han, Y. Zhang and M. Xia, *Sensor Actuat. B-Chem.*, 2015, *212*, 207-213.
39 X. Duan, Z. Ao, H. Sun, S. Indrawirawan, Y. Wang, J. Kang, F. Liang, Z. H. Zhu and S. Wang, *Acs Appl. Mater. Inter.,* 2015, *7* (7), 4169-4178.
40 M. Fan, C. Zhu, Z.-Q. Feng, J. Yang, L. Liu and D. Sun, *Nanoscale,* 2014, *6* (9), 4882-4888.
41 Z. S. Everett C. Salas, Andreas Lu¨ ttge, and James M. Tour, *ACSnano,* 2010, *4* (8), 4852-4856.
42 M. Zhang, X. Mao, C. Wang, W. Zeng, C. Zhang, Z. Li, Y. Fang, Y. Yang, W. Liang and C. Wang, *Biomaterials,* 2013, *34* (4), 1383-1390.
43 G. Xu, B. Li, X. T. Cui, L. Ling and X. Luo, *Sensor Actuat. B-Chem.*, 2013, *188*, 405-410.
44 Y. Xiao, J.-Y. Lin, S.-Y. Tai, S.-W. Chou, G. Yue and J. Wu, *J. Mater. Chem.,* 2012, *22* (37), 19919-19925.
45 P.-Y. Chen, C.-T. Li, C.-P. Lee, R. Vittal and K.-C. Ho, *Nano Energy,* 2015, *12* (0), 374-385.
46 Y. Zhou, C. H. Yen, S. Fu, G. Yang, C. Zhu, D. Du, P. C. Wo, X. Cheng, J. Yang, C. M. Wai and Y. Lin, *Green Chem.,* 2015, *17* (6), 3552-3560.
47 Z. Lin, G. H. Waller, Y. Liu, M. Liu and C.-p. Wong, *Nano Energy,* 2013, *2* (2), 241-248.
48 Z. Xu, H. Li, B. Yin, Y. Shu, X. Zhao, D. Zhang, L. zhang, K. Li, X. Hou and J. Lu, *Rsc Adv.,* 2013, *3* (24), 9344-9351.
49 P. H. Matter, L. Zhang and U. S. Ozkan, *J. Catal.*, 2006, *239* (1), 83-96.
50 H. Yan and H. Okuzaki, *Synthetic Met.,* 2009, *159* (21–22), 2225-2228.
51 J.-W. Back, S. Lee, C.-R. Hwang, C.-S. Chi and J.-Y. Kim, *Macromol. Res.,* 2011, *19* (1), 33-37.

52 G. Zotti, S. Zecchin, G. Schiavon, F. Louwet, L. Groenendaal, X. Crispin, W. Osikowicz, W. Salaneck and M. Fahlman, *Macromolecules,* 2003, *36* (9), 3337-3344.
53 D. Aradilla, D. Azambuja, F. Estrany, J. I. Iribarren, C. A. Ferreira and C. Alemán, *Polym. Chem.-UK,* 2011, *2* (11), 2548-2556.
54 H. Ju, M. Kim and J. Kim, *J. Appl. Polym. Sci.* 2015, *132* (24), n/a-n/a, DOI: 10.1002/APP.42107.
55 J. Li, J.-C. Liu and C.-J. Gao, *J. Polym. Res.*, 2010, *17* (5), 713-718.
56 J. O. Hwang, J. S. Park, D. S. Choi, J. Y. Kim, S. H. Lee, K. E. Lee, Y.-H. Kim, M. H. Song, S. Yoo and S. O. Kim, *Acs Nano,* 2012, *6* (1), 159-167.
57 Y. Xu, Y. Wang, J. Liang, Y. Huang, Y. Ma, X. Wan and Y. Chen, *Nano Res.,* 2009, *2* (4), 343-348.
58 S. S. Kumar, J. Mathiyarasu, K. L. N. Phani and V. Yegnaraman, *J. Solid State Electr.,* 2005, *10* (11), 905-913.
59 B. G. Choi, J. Hong, W. H. Hong, P. T. Hammond and H. Park, *Acs Nano,* 2011, *5* (9), 7205-7213.
60 B. You, L. Wang, L. Yao and J. Yang, *Chem. Commun.,* 2013, *49* (44), 5016-5018.
61 B. You, J. Jiang and S. Fan, *Acs Appl. Mater. Inter.,* 2014, 6, 15302-15308.
62 Y. Yan, T. Kuila, N. H. Kim, S. H. Lee and J. H. Lee, *Carbon* 2015, *85*, 60-71.
63 Z.-Y. Yang, L.-J. Jin, G.-Q. Lu, Q.-Q. Xiao, Y.-X. Zhang, L. Jing, X.-X. Zhang, Y.-M. Yan and K.-N. Sun, *Adv. Funct. Mater.,* 2014, *24* (25), 3917-3925.
64 G. Ciapetti, E. Cenni, L. Pratelli and A. Pizzoferrato, *Biomaterials,* 1993, *14* (5), 359-364.
65 M.-M. Song, W.-J. Song, H. Bi, J. Wang, W.-L. Wu, J. Sun and M. Yu, *Biomaterials,* 2010, *31* (7), 1509-1517.
66 X. Sun, Z. Liu, K. Welsher, J. Robinson, A. Goodwin, S. Zaric and H. Dai, *Nano Res.,* 2008, *1* (3), 203-212.
67 X. Zhang, J. Yin, C. Peng, W. Hu, Z. Zhu, W. Li, C. Fan and Q. Huang, *Carbon,* 2011, *49* (3), 986-995.
68 O. N. Ruiz, K. A. S. Fernando, B. Wang, N. A. Brown, P. G. Luo, N. D. McNamara, M. Vangsness, Y.-P. Sun and C. E. Bunker, *Acs Nano,* 2011, *5* (10), 8100-8107.
69 S. Liu, T. H. Zeng, M. Hofmann, E. Burcombe, J. Wei, R. Jiang, J. Kong and Y. Chen, *Acs Nano,* 2011, *5* (9), 6971-6980.
70 O. Akhavan and E. Ghaderi, *Acs Nano,* 2010, *4* (10), 5731-5736.
71 J. C. Carrero-Sánchez, A. L. Elías, R. Mancilla, G. Arrellín, H. Terrones, J. P. Laclette and M. Terrones, *Nano Lett.,* 2006, *6* (8), 1609-1616.
72 M. L. Zhao, D. J. Li, L. Yuan, Y. C. Yue, H. Liu and X. Sun, *Carbon,* 2011, *49* (9), 3125-3133.
73 Y. Lai, C. Xie, Z. Zhang, W. Lu and J. Ding, *Biomaterials,* 2010, *31* (18), 4809-4817.
74 D. Yang, X. Lü, Y. Hong, T. Xi and D. Zhang, *Biomaterials,* 2013, *34* (23), 5747-5758.

Table of contents entry

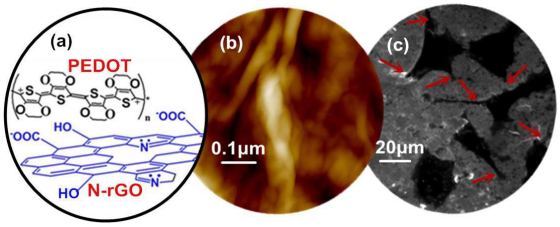

(a) the schematic diagram and (b) AFM image of the surface of PEDOT/N-rGO, (c) the cell morphology cultured on PEDOT/N-rGO.